Institut Laue-Langevin (ILL)

Tutor: Miguel Angel Gonzalez

Author: Alvaro Silva-Santisteban

Short- and intermediate- range order of n-butanol

Introduction

N-butanol is a primary alcohol which enjoys widespread industrial use. In order to better comprehend its properties for further applications it is essential to achieve a complete understanding of its structure. Therefore, the objective of this paper is to determine the short-range order of n-butanol, studying in depth the configuration of the molecules belonging to its first-coordination shell. Furthermore, an attempt to describe the intermediate range order of n-butanol is made by analyzing the topology and geometry of n-butanol clusters.

In the case of short-range order, the six degrees of freedom, i.e. position and orientation in space, of the two nearest molecules around a central one are described. Regarding clusters, several traits were taken into consideration such as size, topology, and the possible appearance of ring-like structures.

The data was obtained from classical molecular dynamics simulation on DL Poly using OLPS-AA force fields. For the simulation, 1000 flexible molecules were used in a unit cell with periodic boundary conditions. In order to carry out simulations at a wide range of temperatures, at each temperature a simulation in the isothermal-isobaric (NPT) ensemble was done first to determine the right size of simulation box, but then actual data was extracted from an isothermal-isochoric (NVT) ensemble, with a Berendsen thermostat. Integration of the equations of motion was done with the leapfrog verlet algorithm with a time step of 1 fs. Ewald summation was used for the electrostatic contributions. A cut-off radius of 12.0 Å for van der Waals forces was used.

Calculations and analysis were done using Angula (developed by LC Pardo) and Numpy (Numerical Python), mainly. Plots and graphs were constructed using Gnuplot, molecular models using Rasmol and Materials Studio.

Short range order /Position and orientation of neighbors

The objective is to gain further knowledge on the short range structure of liquid butanol, especially concerning the OH group. The coordination number is representative of the average number of neighboring molecules around an OH group; to obtain it, we must integrate the radial distribution function which is defined by

$$RDF(r) \stackrel{\text{def}}{=} 4\pi r^2 \rho_o \, g(r)$$

where ρ_o is the volumetric density. Integrating the radial distribution function from the partial pair correlation function $g_{OO}(r)$ with limits at the first two minima, i.e. the first shell, we obtain approximately 2. It is therefore interesting to analyze in detail the position and orientation of the first two molecules in terms of distance from a central molecule.

A coordinate system is defined on each n-butanol molecule using the OH bond as a z-axis. The y axis is the cross product of OH and OC, and the x-axis comes from the cross product of the previous two axes.

$$\hat{z} \stackrel{\text{def}}{=} \overline{OH}$$

$$\hat{y} \stackrel{\text{def}}{=} \hat{z} \times \overline{OC_4}$$

$$\hat{x} \stackrel{\text{def}}{=} \hat{y} \times \hat{z}$$

Having defined the coordinate system, in determining the position of the neighboring molecule (the neighboring coordinate system) spherical coordinates are used.

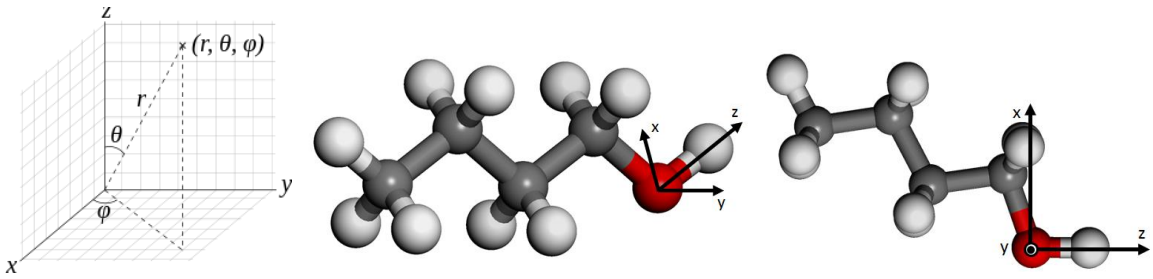

Figure 1. Left: Representation of spherical coordinates convention used. Center and right: Depiction of basis established for each molecule.

Since each molecule has its own coordinate system, the relative orientation of each molecule is best described by calculating the Euler angles, which define the relative orientation of a coordinate system. The Euler convention used here is ZYZ about mobile frame axes (intrinsic rotations), where φ , θ and ψ represent the rotations around the Z, Y', Z'' axes respectively.

In this regard, ψ is the rotation around the molecule's own OH bond, whereas φ is the angle rotated around the OH bond of the central molecule. Finally θ is the value of the angle between both OH bonds (central and neighbor). The φ and ψ angles have a range of values (-180,180], and $\theta \in$ [0,180].

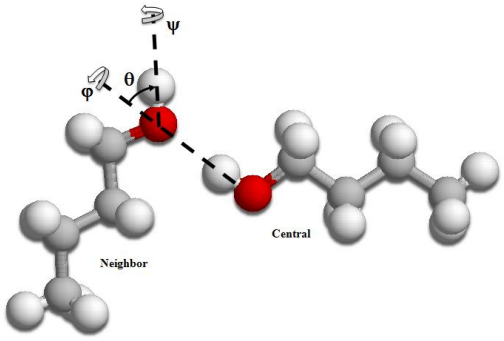

Figure 2. Visual representation of Euler angles. Rotation axes for the neighbor molecule depicted with dashed lines.

To determine the average position of the neighboring molecules, a 3D probability distribution plot is graphed, where the azimuth angle (ψ_o) is plotted against the cosine of the polar angle ($\cos\theta_o$); this latter transformation is used for a better interpretation of the graphs.

An additional two 3D probability distributions plots are used to describe the orientation; the φ and ψ angles are plotted against θ.

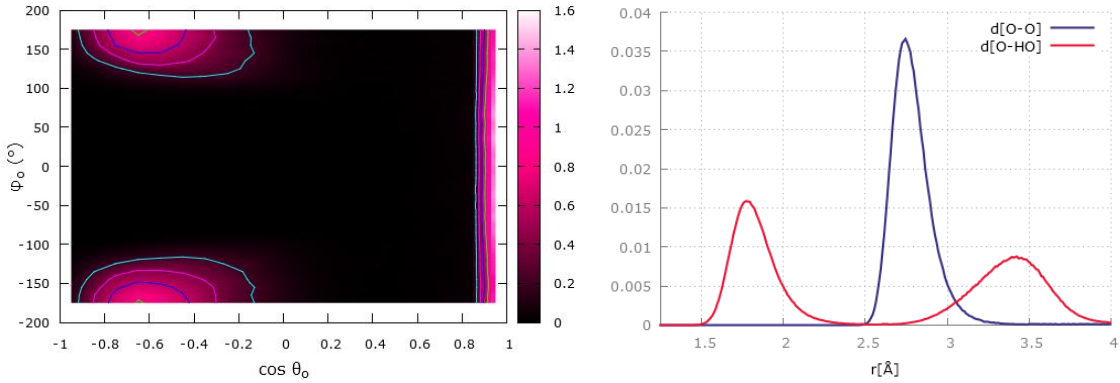

Figure 3. Left: 3D probability distribution plot of position of the oxygen atom of a neighboring molecule. The azimuth angle is the vertical axis and the cosine of the polar angle is the horizontal axis. Right: Distance distributions for the first two molecules. The d[O-O] distribution gives us the radius for the position of the two neighboring molecules. The d[O-HO] distribution has two intervals, one for each of the two neighbors. The interval for O-HO distance of [1.5,2.5] Å is for the molecule positioned at $\cos\theta_o$=1.

Molecule at $\cos\theta_o$=1

The neighboring molecule is in the direction of the OH bond, which is in accordance with the angle restraint pertaining to a hydrogen bond; regarding distance, the O-O distance is in the range of [2.5,3.0] Å (Figure 3 right), which marks plausible distances for hydrogen bonding. For such a value of $\cos\theta_o$, the value of the φ_o angle is meaningless.

Regarding orientation, the θ angle, which describes the angle between the two z-axes (in this case, the two OH bonds), has a restricted range of [36,80]°, which implies a fixed HOH angle. Although the φ angle, which describes the rotation around the OH bond of the central molecule, does not seem to have a restricted range of values, the irregularity of the shape of the plot is probably due to the shape and form of the molecule. The ψ angle seems to have a restricted value around 180°, which is explained by the co-planarity of the OH groups.

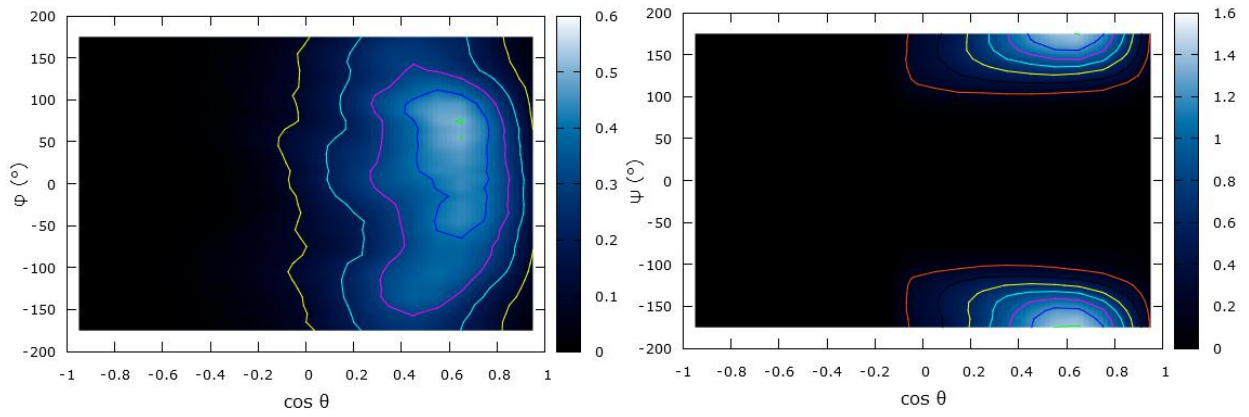

Figure 4. 3D probability distribution plot of orientation of a neighboring molecule in regard to a central one. For a short range of θ values: ψ is fixed and φ can assume a wide range of values, which implies possible mobility of the neighbor around the donor OH bond.

Molecule at cos θ_o ≅ -0.6, or longitude ≅ 125°

Concerning its position, the oxygen atom of the neighboring molecule is positioned on the XZ plane of the central molecule, i.e. the plane defined by C-O-H of the central molecule (φ_o ≅ 180°). This denotes a coplanar short-range arrangement of the OH bonds.

As to its orientation, the second molecule's OH bond has a fixed orientation due to hydrogen bonding. The rotation of the molecule around this OH bond however is not fixed, but seems to display two probable positions at 120° and -120°. This is due to the geometry of the molecule and the impossibility to overlap with the central one.

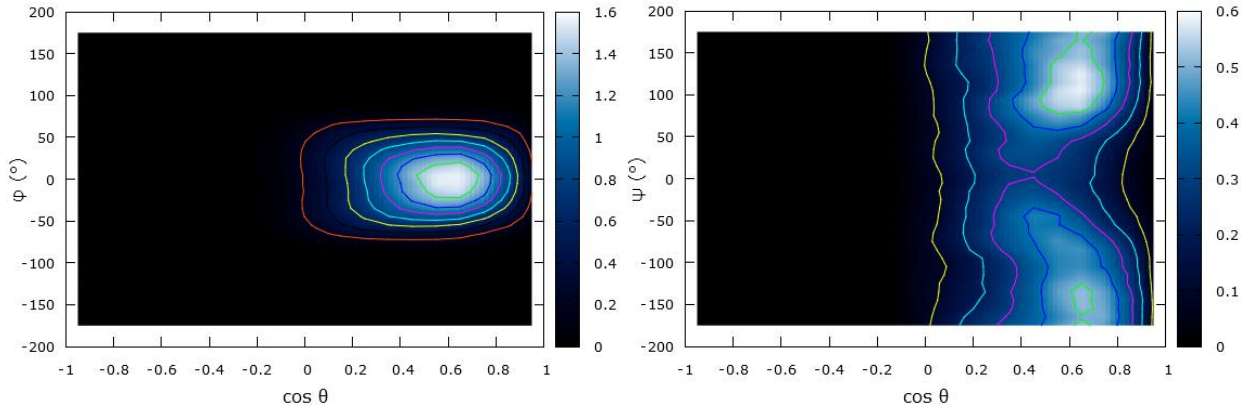

Figure 5. 3D probability distribution plot of orientation

From this we deduce that there is also a fixed HOH angle when a hydrogen bond forms, and that the donor molecule can assume a wide range of orientations around its own OH bond. In addition, the OH bonds in the short range order are coplanar, which would account for an approximately flat or planar cluster formation. This configuration can also be extended to when three hydrogen bonds are formed.

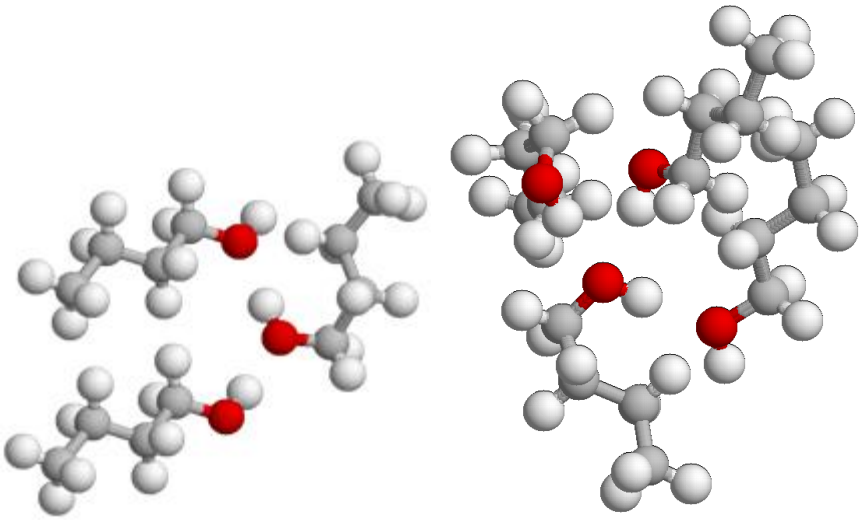

Figure 6. Left: A possible ordering of three n-butanol molecules. Right: A possible ordering of four n-butanol molecules. Note that the OH groups maintain a planar arrangement.

Pair distribution functions and static structure factors

The pair distribution functions and static structure factors help to understand the temperature dependence of the structure of the liquid in study.

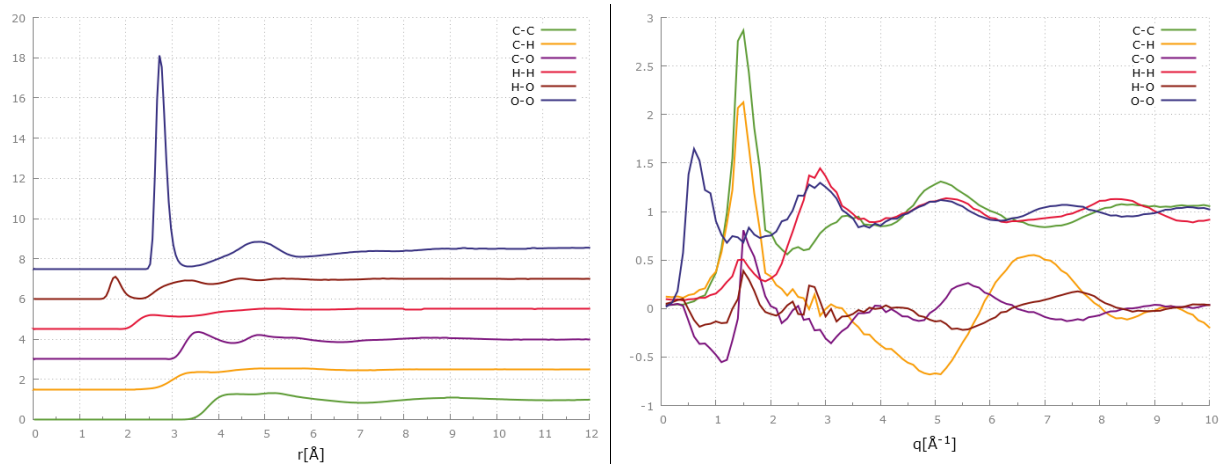

Figure 7. Left: Intermolecular partial pair correlation functions g(r) at 190 K; each has been separated by steps of 1.5. The hydrogen bonding signature can be seen in the strong O-O peak as well as the first and second H-O peaks. Right: Partial static structure factors at 190 K.

The O-O pair distribution function has two easily discernible peaks. The first is due to hydrogen bonding with the immediate neighbors, while the second broader peak is also due to hydrogen bonding but the contribution is by oxygen atoms farther in the "OH-chain" of hydrogen bonds. These oxygen atoms are at a distance of 5.0 Å approximately, depending on the polar angle θ of position; in other words the contribution is of O-O correlation between the neighbor molecules themselves, and not between a central and neighbor molecule, which is the case of the first peak.

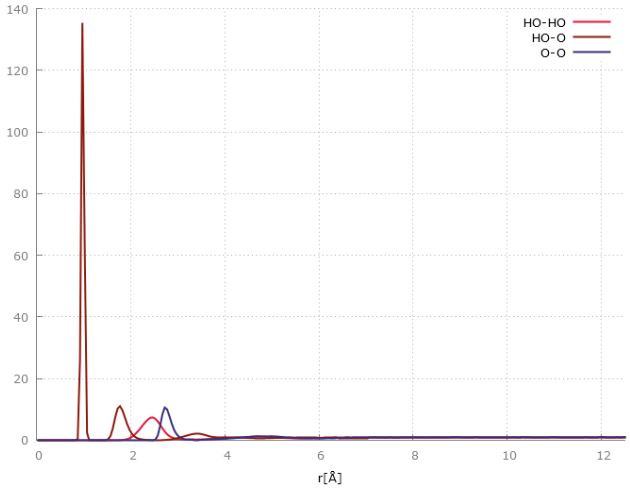

Figure 8. Partial pair distribution functions. Only the two atoms in the OH group were considered. The HO-O g(r) has three peaks; the first is at the intramolecular distance, the second is at the distance for a donor, and the third peak is at the distance for an acceptor. The only O-O peak is at the typical distance for hydrogen bonding.

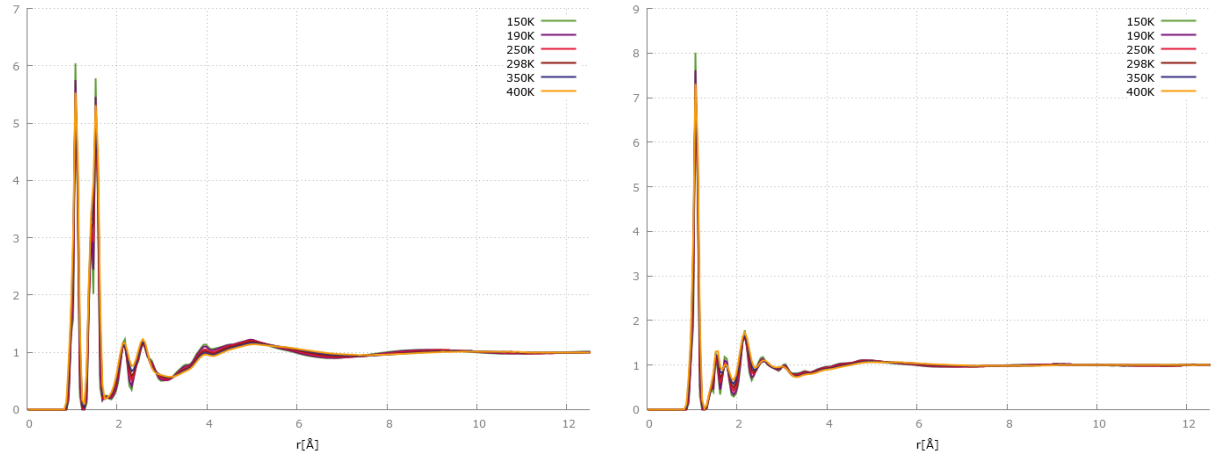

Figure 9. Left: Evolution of the total pair correlation function g(r) with temperature. Atomic numbers were used for weights. Right: Evolution of g(r) with temperature. Deuterated hydrogen was used instead and weighing with the coherent scattering cross-section. The sharp peaks below 2 Å are intramolecular contributions. The peaks from 2 to 3 Å are from hydrogen bonding contributions.

There is a so-called ‘pre-peak’, which appears before the main peak in the static structure factor, which has been said to be the mark of hydrogen bonding [4,5,7]. However, it has been noted that this pre-peak presents anomalous behavior with changing temperature.

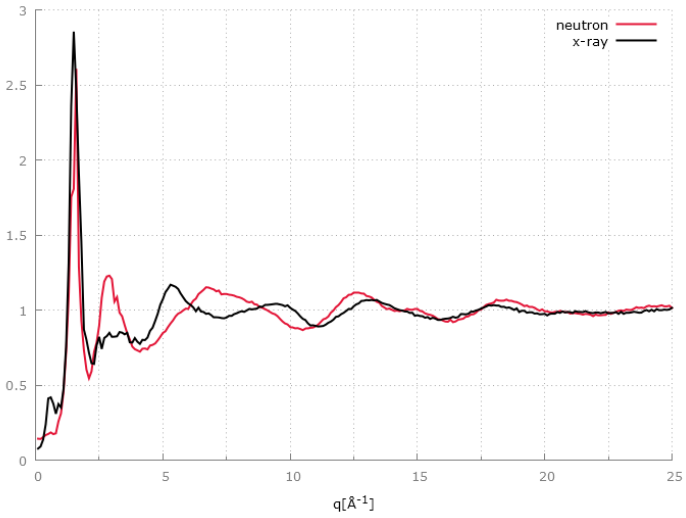

Figure 10. Static coherent structure factors S(q), using atomic numbers (x-ray) and scattering cross-section as weights (neutron). The pre-peak at 0.6 Å^{-1} is clearer using atomic weights.

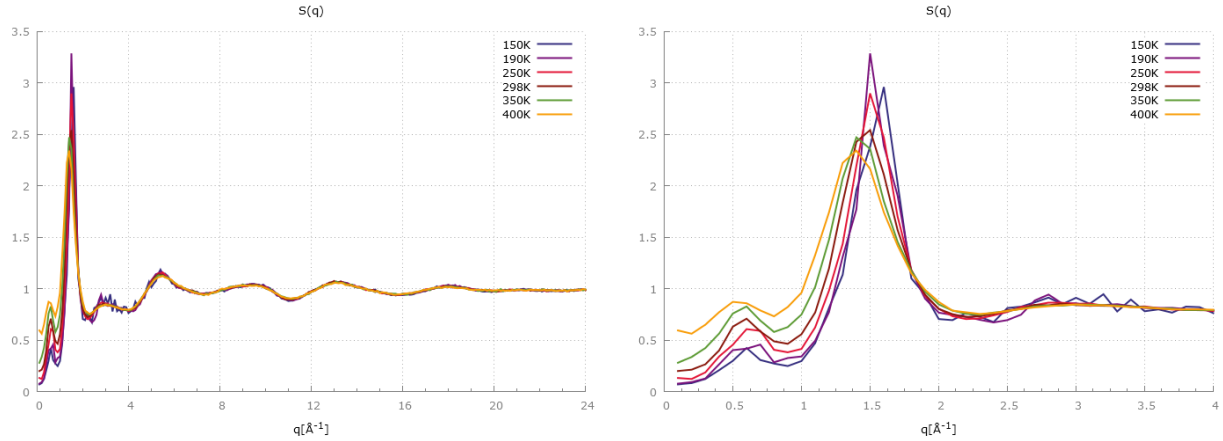

Figure 11. Static coherent structure factor S(q), using atomic numbers as weights, at a range of temperatures. On the right is a zoomed view of the plot on the left, to have a better look at the pre-peak at 0.6 Å^{-1}.

In the static structure factor the pre-peak is at 0.6 Å^{-1} and the main peak at approximately 1.5 Å^{-1}; the pre-peaks main contribution is from the O-O correlation, whereas the main peak contains all partials except O-O (Figure 7 right). The main peak becomes wider and moves toward lower q values, which is regular behavior with increasing temperature. However, the pre-peak evolves differently for it becomes more distinct with rising temperature up to 350 K; this atypical behavior has been thought to be caused by effects in hydrogen bonding [4,5,7].

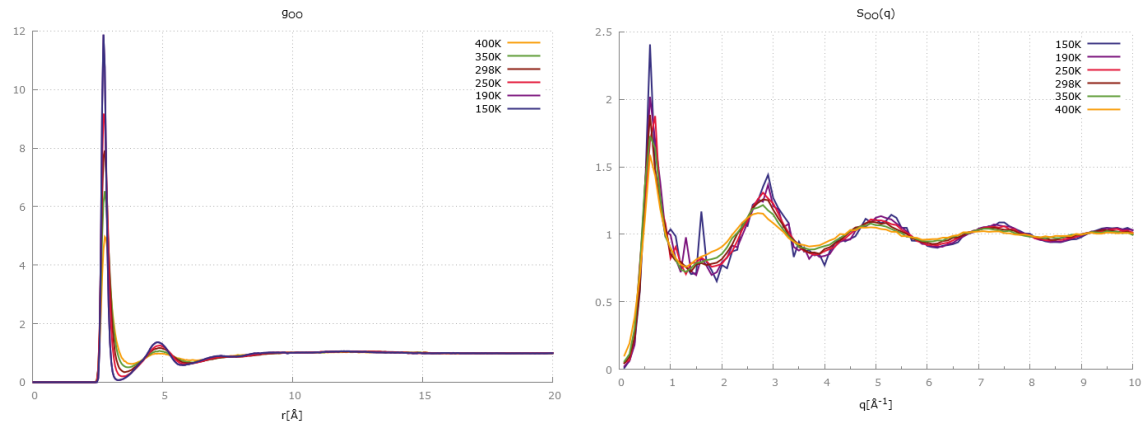

Figure 12. Left: Partial pair distribution function O-O at different temperatures. Right: Partial static structure factor O-O at different temperatures.

As can be seen in Figure 12, the first peak of the static structure factor for O-O evolves with temperature as expected; the peak grows wider and less defined with increasing temperature. Despite the O-O correlation being the main contribution, the pre-peak in the total structure factor evolves differently (Figure 11). Therefore, the behavior of the pre-peak cannot be attributed to a physical behavior of hydrogen bonding. The pre-peak's abnormal changes seem due to contributions of other correlations, mainly C-O and H-O which form a peak at around 0.5 $Å^{-1}$ which intensifies with growing temperature.

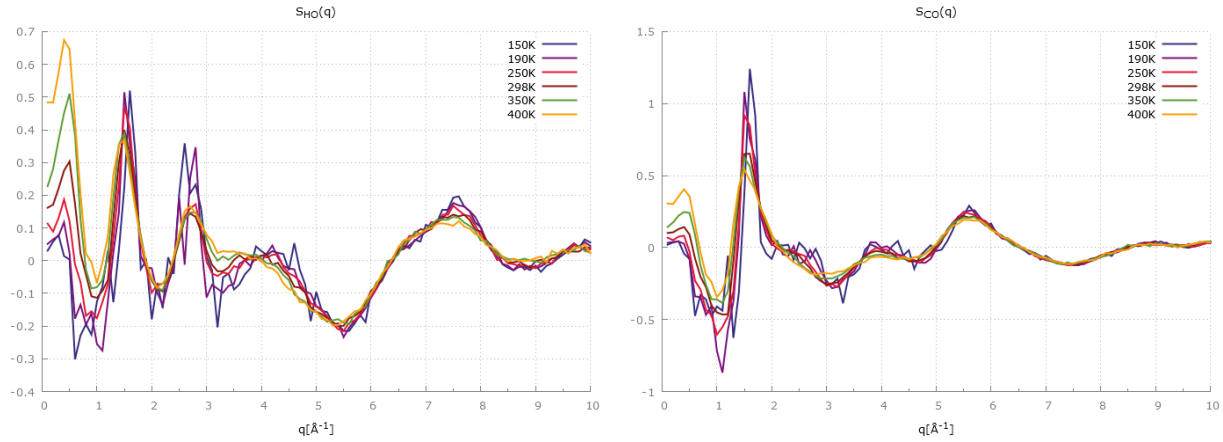

Figure 13. Left: Partial static structure factor H-O. Right: Partial static structure factor C-O. In both plots there is a peak at about 0.5 $Å^{-1}$ which becomes stronger with rising temperature.

However, the anomalous behavior in Figure 13 is not due to effects in hydrogen bonding, as can be seen in Figures 12 and 14, but rather to a sort of intermediate-range order that appears with temperature growth.

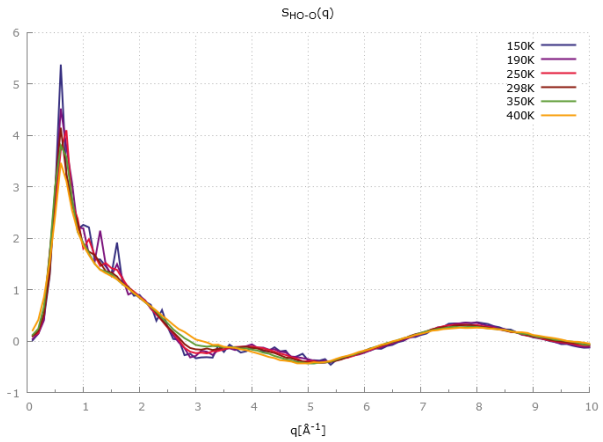

Figure 14. Partial static structure factor HO-O. The first peak behaves as expected with rising temperature.

Intramolecular structure or conformations

In order to carry out the study of the possible conformations in n-butanol, three dihedral angles were taken into consideration: C-C-C-C, C-C-C-O, C-C-O-H. The dihedral angles were calculated from simulation data over n steps, over a range of temperatures. The probability distribution functions of the C-C-C-O, C-C-O-H dihedral angles are quite similar, showing a slight preference for the trans (180°) conformation over the gauche+ (300°) and gauche- (60°) conformations. Nevertheless, this is not the case for the C-C-C-C dihedral angle, in which the trans conformer makes up ~98% of molecules at 190 K.

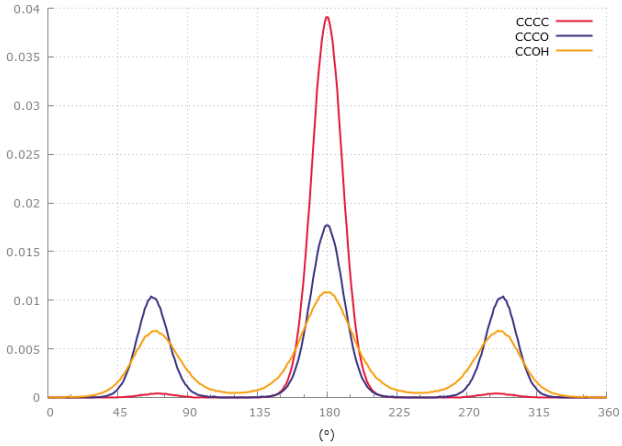

Figure 15. Torsion distributions for N-butanol.

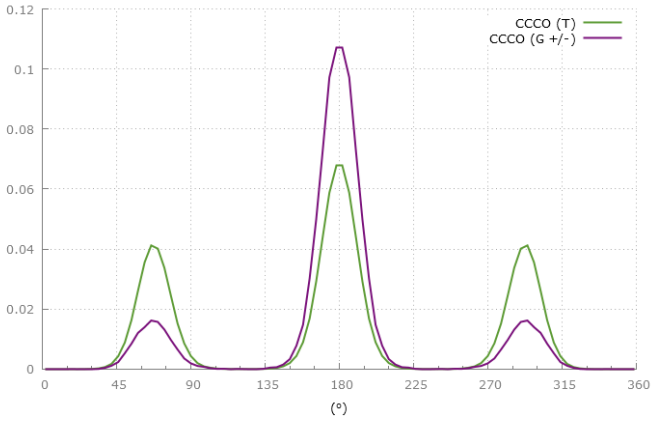

Figure 16. Distributions of C-C-C-O angle. Distribution for a C-C-C-C trans conformation (green) and distribution for a C-C-C-C gauche conformation (purple)

Restricting the values of the C-C-C-C angles we observe different distributions of the same C-C-C-O dihedral angle. With C-C-C-C gauche, there is a considerably greater proportion of C-C-C-O trans than with C-C-C-C trans. Notwithstanding, the C-C-O-H dihedral angle displays an approximately equal distribution of trans, gauche (+) and gauche (-), regardless of restricted values of the other angles.

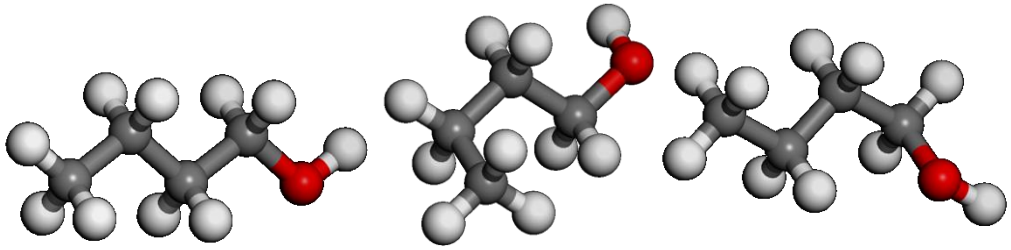

Figure 17. Images depicting different n-butanol conformers: TTT, GTG, and TTG.

Intermediate-range order / Cluster formation

Despite the molecular coordination number of an OH group being approximately 2 on average, it must be considered that each OH group is able to form up to three hydrogen bonds; the oxygen has two lone pairs which act as acceptors and a hydrogen atom as a donor. Therefore although the average number of bonds per OH group is approximately 1.89, this number by itself is not enough to study the topology of the clusters.

A possible approach to studying the OH-clusters is to consider a network or graph of molecules, where each molecule is ‘connected’ if a hydrogen bond exists; each connected subgraph is then a OH-cluster. Each network was constructed using the Python module Networkx, where each molecule is a node and hydrogen bonds are edges. A hydrogen bond is defined with geometric criteria, by an oxygen-oxygen distance of less than 3.0 Å, and an OHO angle range of 150-180°.

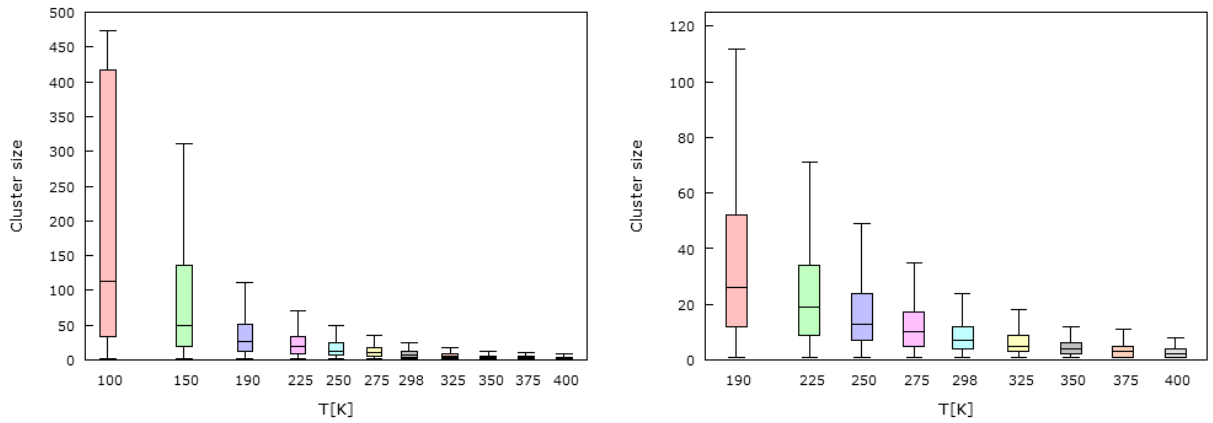

Figure 18. Box plots of cluster sizes at a range of temperatures; the whiskers show the maximum and minimum, the edges of the box are the first and third quartiles, and lines inside the box represent the medians. Outliers were discarded.

The cluster size median does not vary as sharply as the deviation, measured by the first and third quartiles of the box plots (Figure).

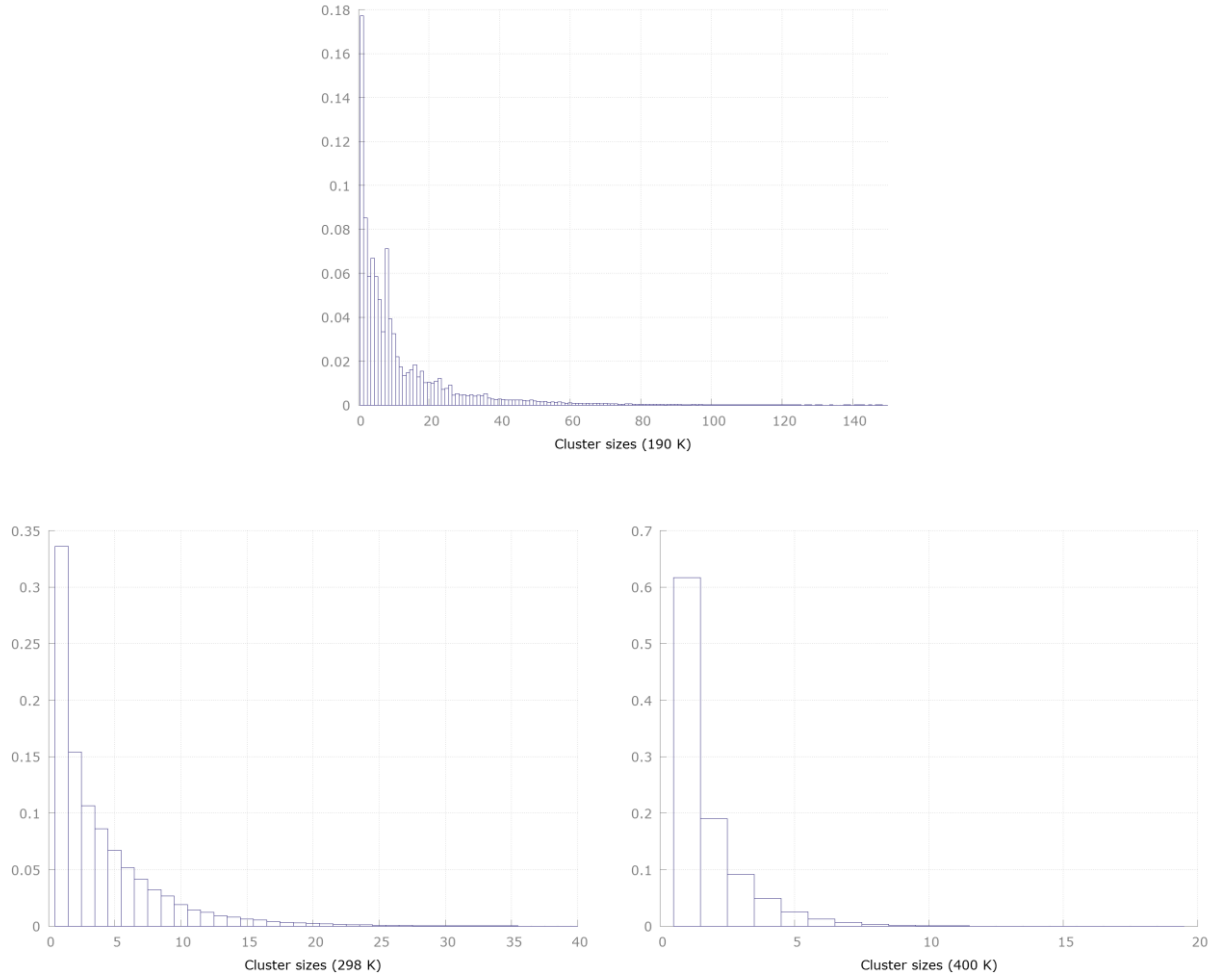

Figure 19. Normalized histograms of cluster sizes at 190K (top), 298K (bottom left) and 400 K (bottom right).

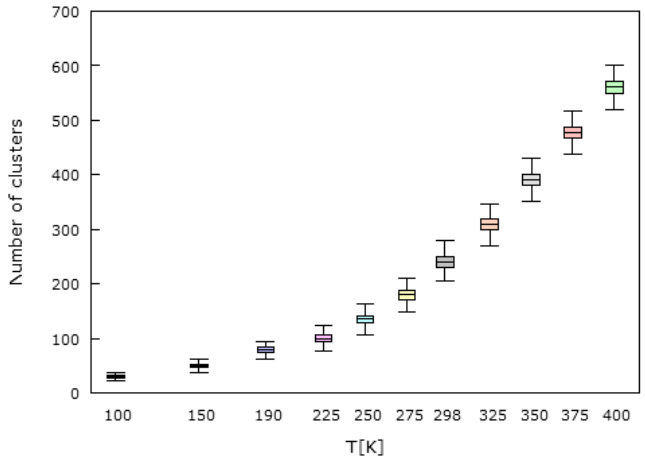

Figure 20. Box plots of the number of clusters displayed as a function of temperature. Same box plot representation as before. Outliers were discarded.

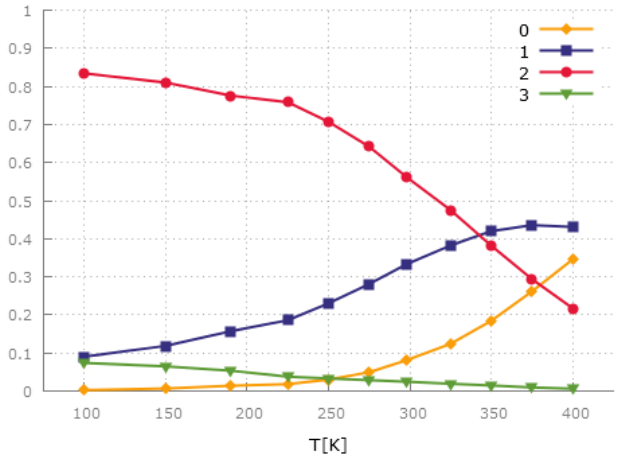

Figure 21. Fraction of molecules with a certain number of hydrogen bonds as a function of temperature. Cluster become more linear with growing temperature.

The topology of the clusters is slightly branched, having 5% of molecules with 3 hydrogen bonds at 190 K. With rising temperature, however, the clusters become more linear as the average coordination number diminishes, which could also be seen in the decrease in cluster size.

An algorithm based on depth-first search was programmed and implemented using Python to determine the number of loops per cluster as well as loop length. Another similar algorithm is also used to distinguish the clusters as connected subcomponents of a larger network. These loops can be either lone rings and be a separate cluster, i.e. loop size equivalent to cluster size, or loops within a larger cluster, as “lassos” [1].

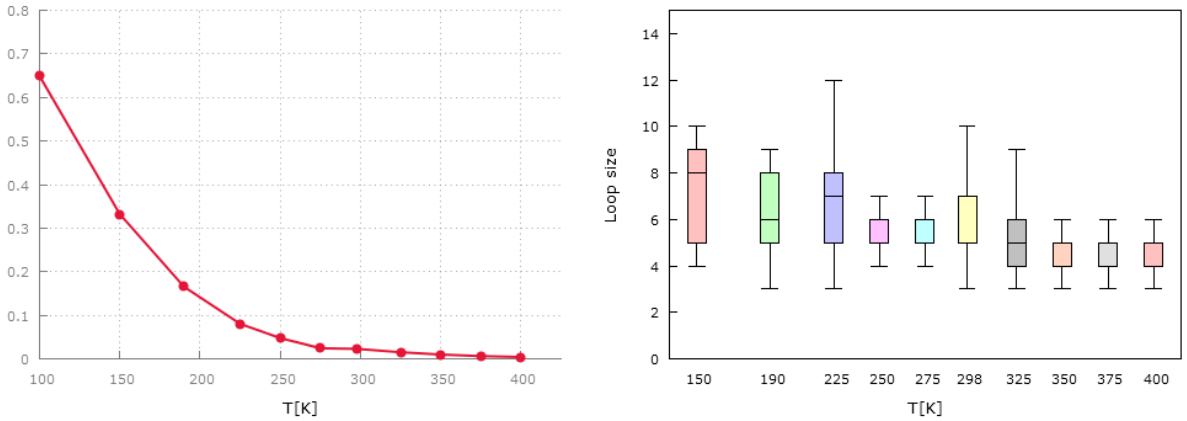

Figure 22. Left: Fraction of clusters with at least one loop or ring-like structure. Right: Box plots of loop size. Outliers were discarded. No clear pattern with temperature variation can be seen.

There is a considerable number of clusters with ring-like formation, as many as 20% at 190K. Nevertheless, it is very rare to find more than one loop per cluster. Concerning loop length, the mean is approximately constant for varying temperatures, at around 7 molecules, however it behaves abnormally. This loop formation is especially interesting since it has not been taken into consideration in past statistical model for hydrogen bonding of alcohols [1,2].

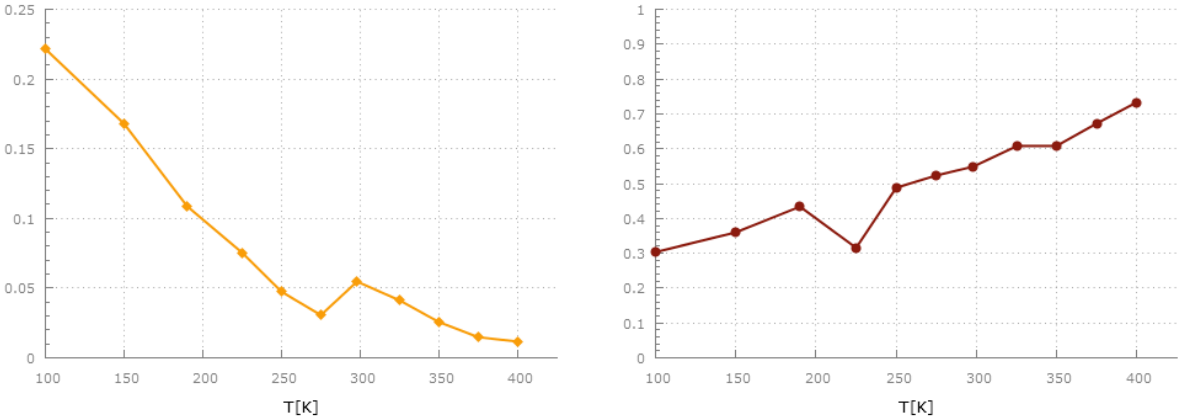

Figure 23. Left: Percentage of n-butanol molecules found in a closed loop, displayed as a function of temperature. Right: Percentage of loops that are separate rings, as a function of temperature.

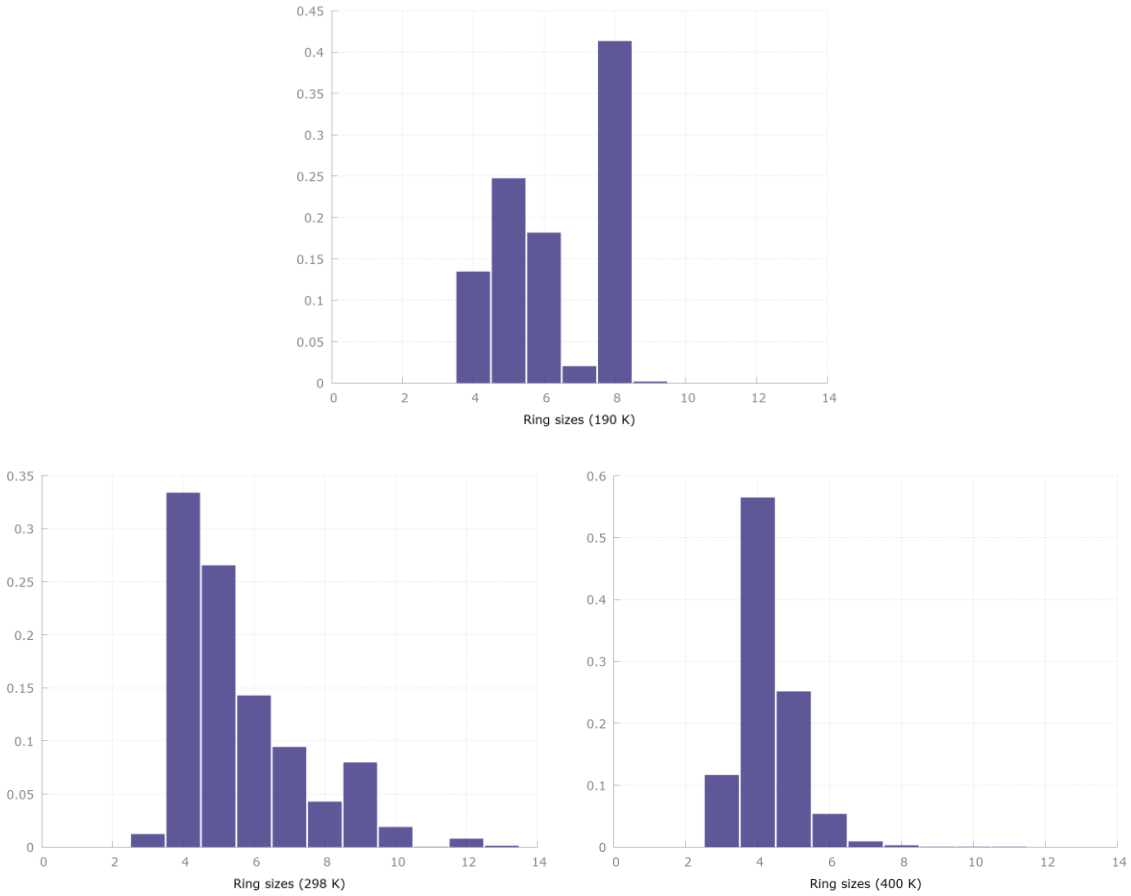

Figure 24. Size distribution of lone rings at 190 K, 298 K and 400 K.

Hydrogen bond lifespan

The mean lifespan of a hydrogen bond having been found to be in the order of 10^{-11} s [1], it is plausible to determine its temperature dependence using simulation data, as the graphs are calculated every 0.2 ps for a total of 200 ps, leaving a relative error of a centesimal order. Bearing in mind the geometric definition of a hydrogen bond (O-O distance under 3.0 Å and OHO angle between 150° and 180°), a hydrogen bond is considered to have broken as soon as it stops fulfilling the definition.

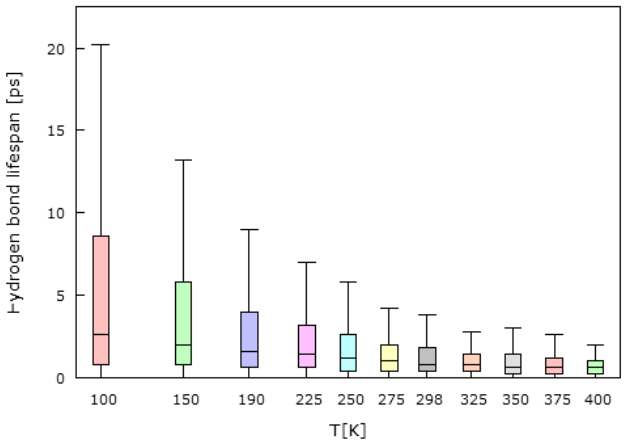

Figure 25. Box plots of lifespan of a hydrogen bond, as a function of temperature.

Hydrogen bond lifespan's mean and deviation lowers with rising temperature; the median however does not decrease as drastically. The values are $\sim 10^{-10} - 10^{-12}$ s.

Diffusion coefficient

The coefficient for isotropic and unhindered translational diffusion is deduced from the mean squared displacement $\langle (\Delta r)^2 \rangle$ of a particle in Brownian motion, which obeys the following equation in the case of three dimensional Brownian motions

$$\langle (\Delta r)^2 \rangle = 6 \cdot D \cdot \Delta t$$

Therefore, the diffusion coefficient for each temperature was calculated by performing a linear fit of the mean squared displacement over time, and dividing the resulting slope by six. The mean squared displacement was calculated using nMoldyn.

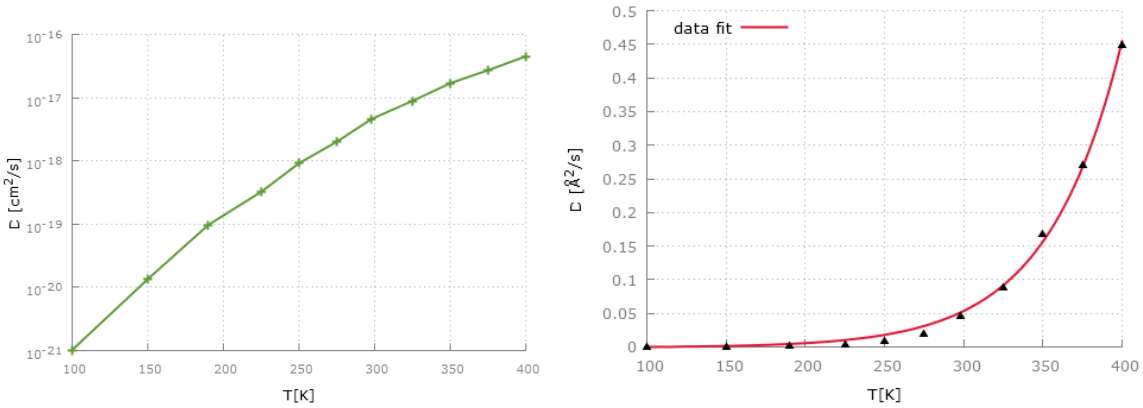

Figure 26. (left) Plot of diffusion coefficients over a range of temperatures. (right) Fitting of diffusion coefficient data. Triangles are simulation data.

$$f(T) = a \cdot [e^{b \cdot (T-100)} - 1]$$

Using the equation above and fitting parameters a, b using nonlinear least squares regression, the values $a = 0.000770\ K^{-1}$, $b = 0.021273\ \frac{\text{Å}^2}{s}$ were obtained.

Density as a function of temperature

The density calculated from simulation data naturally diminishes with growing temperature. However, it evolves differently depending on the temperature range; the inflection point is the glass transition temperature T_g^*. This T_g^* is significantly greater than the T_g found experimentally however, due to the simulation times (400 ps) being of a much lesser order than the relaxation time considered when calculating the experimental T_g (~100 s).

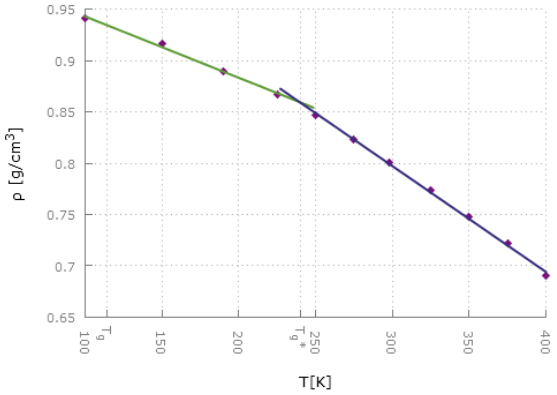

Figure 27. Density plotted as a function of temperature. The T_g^* for simulations tends to be much higher than that found through experimental procedures. T_g=114 K [3]. Diamonds represent the data and solid lines represent trends in density evolution.

Conclusions

In the short-range order there seems to be a somewhat fixed arrangement concerning the OH groups due to hydrogen bonding; the OH groups are in a planar configuration, with relatively fixed angles among each other. In addition, the coordination number of the OH groups can vary from 0 to 3, according to the number of hydrogen bonds that have been formed.

This configuration in the short-range order extends to geometric properties of clusters in the intermediate-range order. A coordination number of 3 leads to branched structures of clusters, and in some cases ring-like formations. However, the topology of the clusters grows linear with increasing temperature. Furthermore, the planar arrangement extends to the shape of the clusters, as they are relatively flat; this result was contrasted performing *ab initio* simulations between small groups of molecules. The cause of the anomalous behavior of the 'pre-peak' in the static structure factor is due to a sort of intermediate-range order not directly related to hydrogen bonding, but has yet to be fully determined.

Acknowledgements

I would like to thank the ILL for giving me this internship opportunity. I would also like to thank my tutor Miguel Angel Gonzalez for instruction and support, and Luis Carlos Pardo for counsel and allowing use of his program.

Appendix

Euler angles

They are calculated using the following formulae

$$\varphi = \frac{z_y}{|z_y|} \cdot \arccos \frac{z_x}{\sqrt{1 - z_z^2}} \quad (1) \qquad \theta = z_z \quad (2) \qquad \psi = -\frac{y_z}{|y_z|} \cdot \arccos \frac{-x_z}{\sqrt{1 - z_z^2}} \quad (3)$$

where z_y stands for the projection of the new z-axis on the initial y-axis, and so forth.

The rotation matrix for intrinsic ZYZ rotations, which was used to display the molecules on *Rasmol*, was calculated with

$$[R] = \begin{bmatrix} \cos\varphi & -\sin\varphi & 0 \\ \sin\varphi & \cos\varphi & 0 \\ 0 & 0 & 1 \end{bmatrix} \begin{bmatrix} \cos\theta & 0 & \sin\theta \\ 0 & 1 & 0 \\ -\sin\theta & 0 & \cos\theta \end{bmatrix} \begin{bmatrix} \cos\psi & -\sin\psi & 0 \\ \sin\psi & \cos\psi & 0 \\ 0 & 0 & 1 \end{bmatrix}$$

Diffusion coefficient

The coefficient for isotropic and unhindered translational diffusion is deduced from the mean squared displacement $\langle (\Delta r)^2 \rangle$ of a particle in Brownian motion, which is defined by

$$(\Delta r_i(\Delta t))^2 = (\Delta x_i(\Delta t))^2 + (\Delta y_i(\Delta t))^2 + (\Delta z_i(\Delta t))^2$$

$$\langle (\Delta r(\Delta t))^2 \rangle = \frac{1}{n} \sum_{i=1}^{n} r_i^2(\Delta t)$$

where $\Delta x_i(\Delta t)$, $\Delta y_i(\Delta t)$ and $\Delta z_i(\Delta t)$ are the components of displacement in a time interval of Δt for every i-step. The following equation is true for said three dimensional Brownian motions

$$\langle (\Delta r)^2 \rangle = 6 \cdot D \cdot \Delta t$$

In which D is the diffusion coefficient. Translational diffusion is defined by the following differential equation

$$\frac{\partial \rho(\vec{r})}{\partial t} = D \cdot \Delta \rho(\vec{r})$$

where $\rho(\vec{r})$ is the particle location distribution and Δ is the Laplace operator. The diffusion coefficient for each temperature was calculated by performing a linear fit of the mean squared displacement over time, and dividing the resulting slope by six.

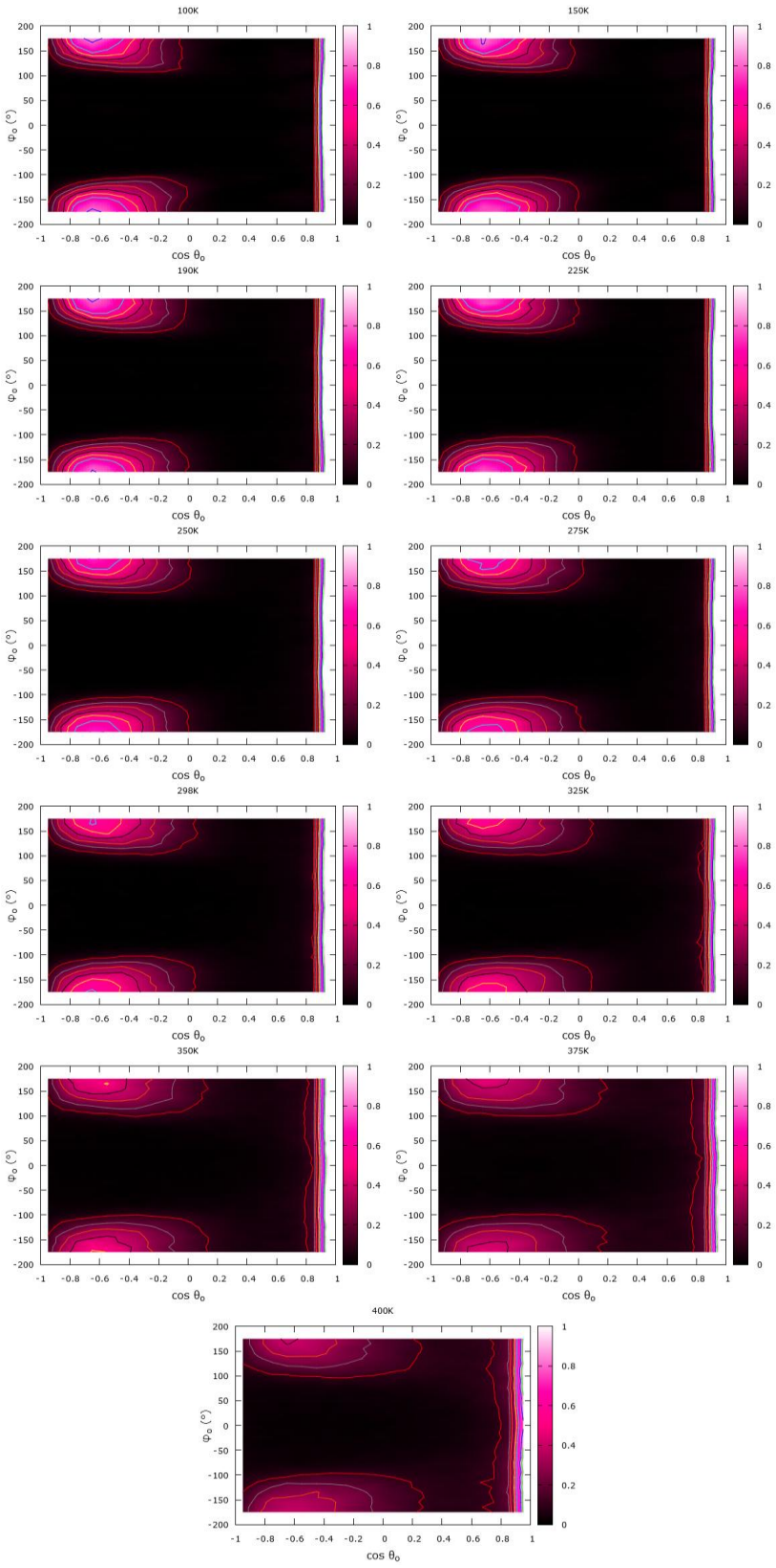

Figure 1. 3D probability distribution plots of position at different temperatures.

References

[1] Per Sillrén, Jan Swenson, Johan Mattsson, Daniel Bowron, and Aleksandar Matic, J. Chem. Phys. **138**, 214501 (2013)

[2] Per Sillrén, Johan Bielecki, Johan Mattsson, Lars Börjesson, and Aleksandar Matic, J. Chem. Phys. **136**, 094514 (2012)

[3] S. Yu. Grebenkin and V. M. Syutkin, PHYSICAL REVIEW B **76**, 054202 (2007)

[4] G. J. Cuello, V. Cristiglio, M. A. Gonzalez, and C. Cabrillo, J. Physics: Conference Series (accepted)

[5] D. Morineau, C. Alba-Simionesco, M.-C. Bellissent-Funel and M.-F. Lauthie, Europhys. Lett., **43** (2), pp. 195-200 (1998)

[6] William L. Jorgensen, David S. Maxwell, and Julian Tirado-Rives**,** *J. Am. Chem. Soc.* **1996,** *118,* 11225-11236

[7] I M Shmytko, R J Jimenez-Rioboo, M Hassaine and M A Ramos, J. Phys.: Condens. Matter **22** (2010) 195102 (9pp)